EVS32 Symposium
Lyon, France, May 19-22, 2019

DC-Link-Capacitor Packaging and Thermal Management for 48-V Hybrid Passenger Vehicles

Yuya Tamai[1], Yuhei Kobayashi[1],Toshiki Wakabayashi[1], Toshihiko Furukawa[2]

[1]*Nippon Chemi-Con Corporation, Japan*

[2] *United Chemi-Con, Inc., 5651 Dolly Ave Buena Park, CA, USA tfurukawa@chemi-con.com*

Summary

A DC-link capacitor module using Nippon Chemi-Con HXC-series capacitors in a novel design is described. The design minimizes resistance and improves thermal efficiency. The thermal properties during operation are simulated under dc and ripple-current conditions for an individual capacitor and for a 48-capacitor module. Model results are compared to experimental temperature measurements and then used to evaluate thermal conditions and to predict module life.

Keyword: 48-V MHV, DC-Link capacitors, Thermal simulation, Thermal management, Life

1 Introduction

To reduce greenhouse gas emissions, costs, and improve fuel economy electric vehicles are projected to reach 70% of global automobile production by 2030 with almost one-half of these being 48-V mild hybrid vehicles (MHVs)[1,2]. Estimated power requirements for next-generation 48-V MHVs are 15 to 25 kW[1, 3]. All 48-V MHV configurations include a motor/generator (M/G) and an inverter module to connect the M/G to the 48 V and 12 V batteries. The DC-link capacitor module is a key elements of the inverter module.

Performance of the DC-link capacitor module depends on the capacitors and on the design of the bus bar on which the capacitors are mounted. Key considerations for the bus bar design are its equivalent series inductance (ESL) and its equivalent series resistance (ESR). The ESL is important because voltage pulses generated during high-current switching must not exceed the inverter voltage rating. The ESR affects losses and thus the heat generation rate and ultimately, system operating efficiency. Also, the life of the module depends directly on the temperatures experienced by the capacitors.

Thermal performance of the capacitor module is investigated with a combination of modeling and experimental measurements of 1) temperature rise during high-current operation, 2) temperature rise in a single capacitor due to ripple current, and 3) temperature of each capacitor in the module due to ripple current. This approach allows evaluation of the thermal management system and permits prediction of module operating life. The new concept bus bar described here is able to provide a suitable design solution for the mild hybrid vehicle application. Details follow.

1.1 Hybrid System and New Concept Bus Bar

A basic block diagram for a 48-V mild hybrid power system is shown in Figure 1. The DC-link capacitor module consists of 48 Nippon Chemi-Con SMD chip-type hybrid polymer aluminum electrolytic HXC-series capacitors (82 µF/63 V). These capacitors have a diameter of 10 mm and a height of 10 mm and are capable of handling high ripple-currents.

The capacitors are mounted on the bus bar as shown in Figure 2 using a novel design that minimizes resistance between the capacitor and the bus bar. The bus bar configuration is sandwich style: the upper and lower sides are each 2 mm thick copper with thermal conductivity of 372 W/m·K. There is a thin sheet of insulating film between the two sides. The film material is FR4 film (L-6505) with a thermal conductivity of 0.5W/m·K.

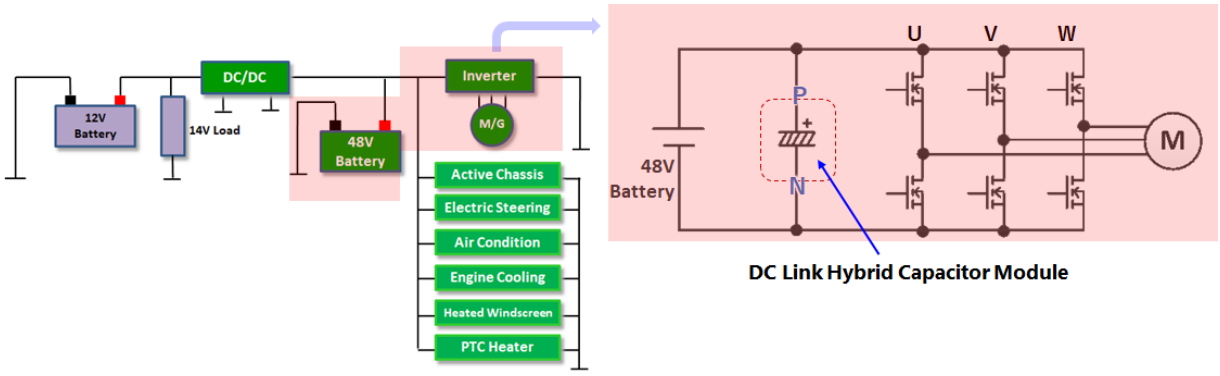

Figure 1: System block diagram for a 48-V mild hybrid passenger vehicle.

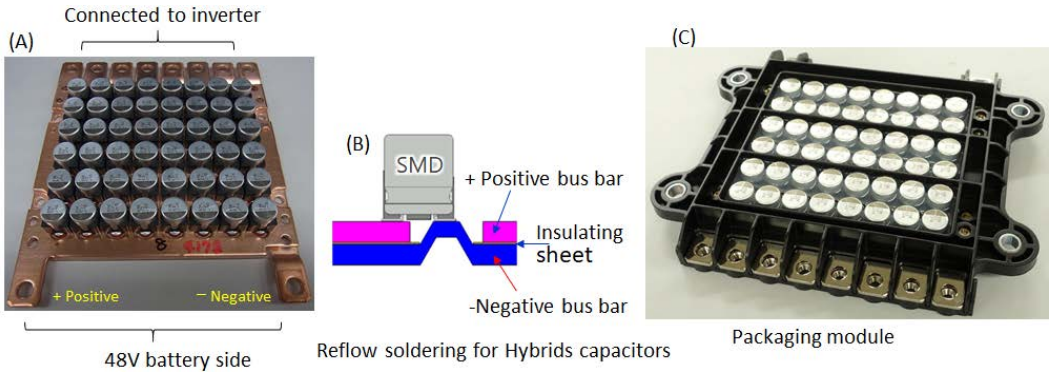

Figure 2:DC-link capacitor module: (A) Photograph of the 48 parallel-mounted capacitors on the 2-mm-thick new concept copper bus bar, (B) Capacitor mounting details (patent pending), and (C) Photograph of the DC-link capacitor module packaging.

1.2 Heat Generation During High-Current Operation

During operation of the 48-V MHV, current can be 300 A or greater. High current can cause excessive heat generation if system resistance is not kept low so it is important to minimize the ESR of the capacitor module while maintaining an acceptably low ESL. Bus bar ESR is calculated as

$$\mathrm{ESR} = \rho \frac{l}{tw} \qquad (1)$$

where ρ is bus bar resistivity, l its length, t its thickness, and w its width [4]. Dynamic power loss P caused by the ESR is $P = I^2 * ESR$ where I is the bus bar current. The bus bar temperature rise due to self-heating is

$$\Delta T = I^2 \cdot ESR \cdot R_{th} \qquad (2)$$

where R_{th} is the effective thermal resistance between the bus bar and its environment. Thus, bus bar temperature rise depends on the current, the bus bar material, and its dimensions.

The temperature of the bus bar with and without capacitors was investigated using dc current instead of the usual ripple current seen during operation, which allowed evaluation of the thermal simulation. Figure 3 shows predicted temperature as a function of applied current from numerical simulations. Predicted temperature as a function of position on the bus bar is also shown for 300 A_{dc} for two different types of connection to the terminals. Current density and thus temperature are highest at the bus bar terminal and local temperatures are higher when current passes through a smaller-area cross-section as shown in Figure 3A than when current is applied using a larger, lower-current density connectionas shown in Figure 3B.

Figure 4 shows temperature measurements during application of 100 A_{dc}, 200 A_{dc}, and 300 A_{dc} through the bare bus bar and a bus bar mounted with capacitors. Connection of the current source to the bus bar was made using three 0000-size copper cables (11.5mm diameter) attached to a 25-mm-wide x100-mm-long x 3-mm-thick aluminum connector strip.

The reason why a connector strip and heavy cables as shown in Figure 3B were added was to simulate actual use. Figure 3C shows current versus temperature at locations T1, T2 and T3 in Figure 3B.

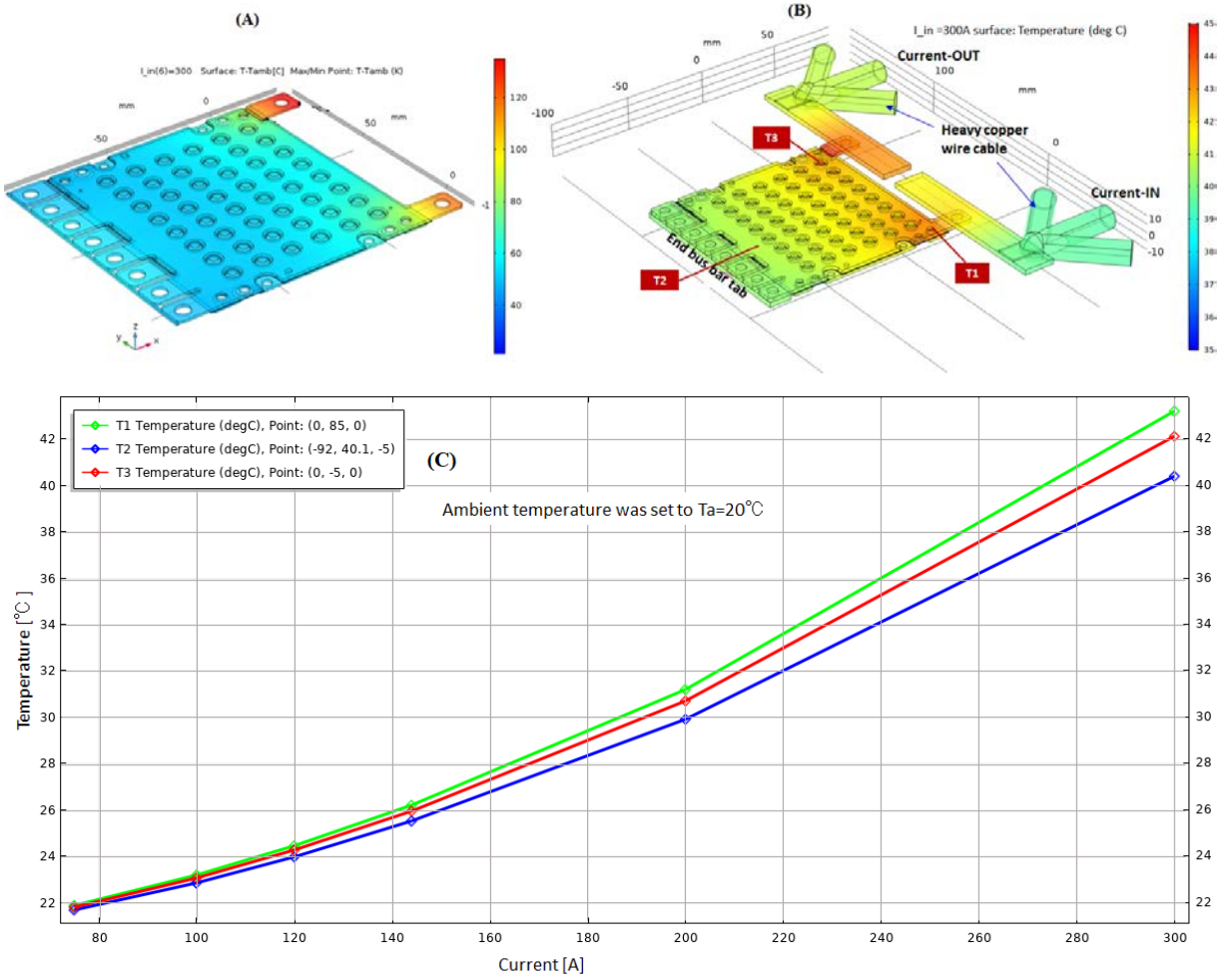

Figure 3: (A) Predicted temperature distribution without heavy cables or connector strip attached to the terminals. (B) Predicted temperature distribution with heavy cables attached to the connector strips that are attached to the bus bar terminals. (C) Predicted temperatures at locations T1, T2 and T3 on the bus bar shown in (B) as a function of applied dc current. Ambient temperature was 20 ºC in these simulations.

Experimentally measured temperatures shown in Figure 4B, which are very close to temperatures predicted by numerical simulation shown in Figure 3, demonstrate that the model is suitable for temperature predictions and can be used to design the bus bar.

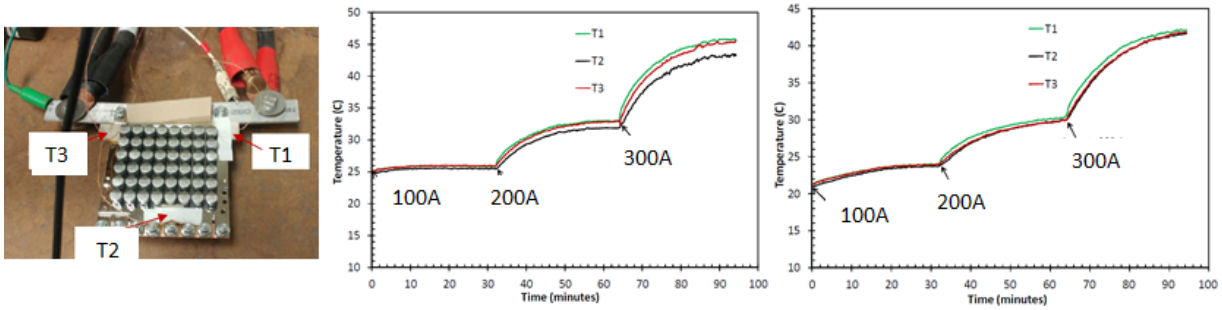

(A) Measurement set up with capacitors on the board

(B) Results with no capacitors on the board

(C) Results with 48 capacitors mounted on the board

Figure 4: (A) Setup for measurement of temperature at three positions on bus bar with 48 capacitors for applied currents of 100 A_{dc}, 200 A_{dc} and 300 A_{dc}. (B) Temperatures at locations T1, T2 and T3 without capacitors on the board. (C) Temperatures at locations T1, T2 and T3 with capacitors on the board. With capacitors, temperature at location T2 is the same as at T3.

Figure 5 shows a photograph of the capacitor temperature measurements with thermocouples on selected capacitors and a thermal image of the bus bar with capacitors. Temperature rise for individual capacitors, listed in Table 1,was measured after current had been applied for 45 minutes when temperatures had reached a steady state value. The thermal image shown was captured after 300 A_{dc} had been applied for 45 minutes. Capacitors closest to the terminals and those on the right side of the bus bar reached higher temperatures probably because of slightly higher current density. Temperatures measured for selected capacitors are shown in Table 1 and graphically in Figure 6. The maximum difference in temperatures between capacitors with 300 A_{dc} applied is ≈3℃.

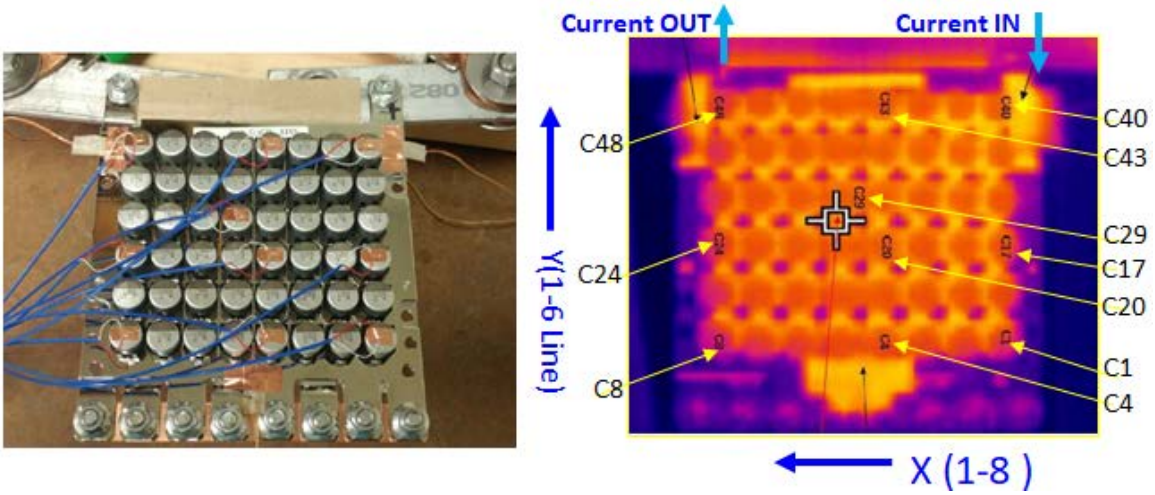

Figure 5: Left – photograph showing thermocouples on the top of selected capacitors. Right - thermal image showing the measurement locations.

Table1: Temperature rise above ambient (~23 ºC) for the selected capacitors shown in thermographic image on the right of Figure 5.

	C1	C4	C8	C17	C20	C24	C 29	C40	C43	C48	Ave	Max	Min	Max-Min
100Adc	2.01	2.01	1.63	2.05	2.09	1.78	2.08	2.1	2.1	1.76	1.961	2.1	1.63	0.47
200Adc	9.56	9.64	8.36	9.91	10.02	8.89	10.04	10.01	10.02	8.9	9.535	10.04	8.36	1.68
300Adc	21.5	21.6	19.42	22.04	22.6	20.42	22.58	22.12	22.5	20.28	21.506	22.6	19.42	3.18

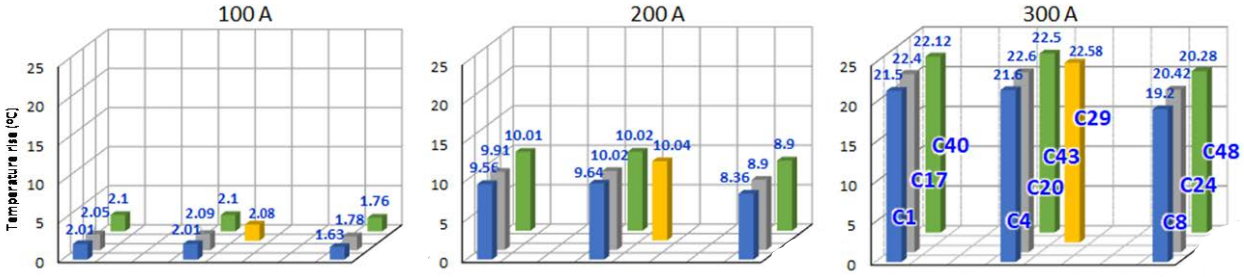

Figure 6: Graphical representation of the temperature rise above ambient of selected capacitors as listed in Table 1. Capacitors positions are as defined in Figure 5.

2 Simulation and Thermal Management

2.1 Single Capacitor Thermal Simulation and Test Data

Another aspect of thermal performance relates to capacitor self-heating caused by ripple-current. The first step in this evaluation was to perform modeling and simulation of a single capacitor. This model was tuned until it accurately predicted experimental temperature data. Model details including thermal parameters of the capacitorare shown in Figure 7 along with a cutaway of a capacitor, which is not isotropic. Additional thermal parameters used in the model are listed in Table 2.

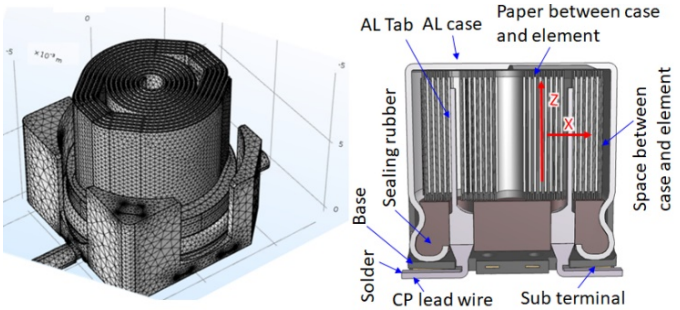

(A) **(B)**

Capacitor thermal simulation parameters

(C)

	Material	Thermal conductivity (W/m.K)	Emis-sivity
Capacitor	Inside material (X-axis)	1.0	0.60
	Inside material (Z-axis)	100	
	Al case and AL Tab	237	
	Paper	0.2	
	CP lead wire	80	
	Sealing rubber and Base	0.2	
	Sub terminal	401	

Figure 7: (A) Mesh for numerical simulation of a single capacitor. (B) Cutaway of the HXC 63V/82µF (ϕ10x10mm) capacitor showing its construction and materials. (C) Table listing the parameters used for thermal simulations.

Table:2 Thermal parameters used for model simulations.

	Material	Thermal conductivity (W/m.K)
Cable	ϕ 0.5 mm Sleeve	0.2
	Multi-Stand copper wire	401
PC board	FR4	0.45
	Copper trace≈56 µm	401
	Solder	49

For the measurements, thermocouples were placed inside the capacitor and along its top and side. The single capacitor was mounted on a PC board 23 mm x 13 mm x 2 mm thick. Temperatures were measured as a function of ripple current up to 5 A. Details of those measurements are shown in Figure 8.

Figures 9 and 10 show results of the thermal simulation of a single capacitor. Table 3 shows a comparison of the simulation with the temperature measurements. Agreement was sufficiently good to allow initial design of the thermal management system.

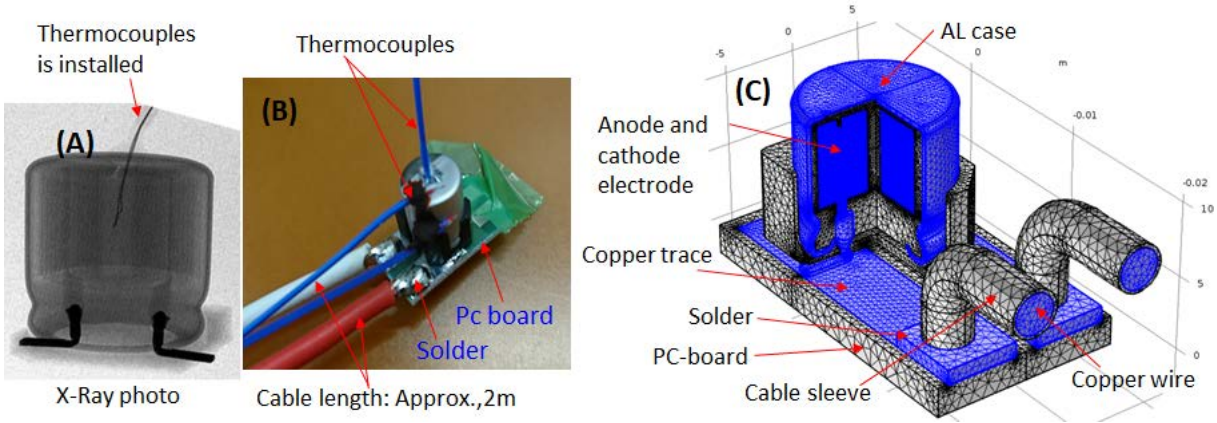

Figure 8: (A) X-Ray photograph of a capacitor with the inserted internal thermocouple. (B) Photograph of the capacitor mounted on PC board with thermocouples attached. (C) Mesh used for numerical simulation of capacitor temperatures when a capacitor was mounted on the PC board.

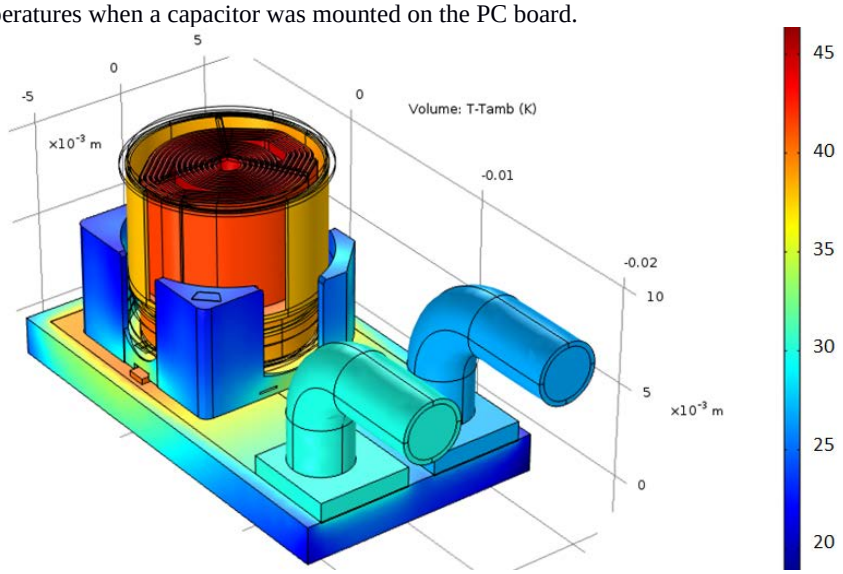

Figure 9: Self-heating, ΔT simulation results for 5 A_{rms} ripple-current. The temperature scale is in °C.

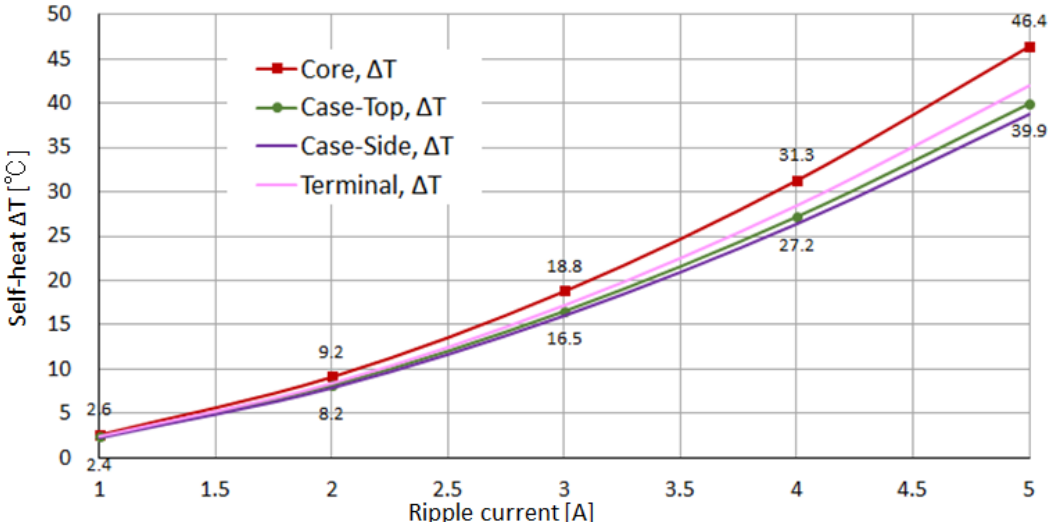

Figure10: Simulated self-heating temperature as a function of ripple-current for the capacitorcore, case-top and case-side.

Table 3: Comparion of simulated and measured termperatures for a 5 A ripple-current.

Thermocouple Location	Temperature (℃)	
	Test Measurements	Simulation Result
Capacitor Core	46.6	46.9
Case Top	39.0	40.6
Case Side	37.2	38.1

2.2 The Need for Thermal Management in a 48-Capacitor Module

The invertor switching frequency of this 48-V MHV is 10 kHz. Module ripple-current was 90 to 130 A_{rms} in this study. The current rating of one HXC series 82 µF/63 V capacitor is ≈1.0 A_{rms} at 10 kHz. Then in a module of 48 capacitors mounted in parallel the current per capacitor ranges from 90 A_{rms}/48≈2.0 to 130 A_{rms}/48 ≈3.0 A_{rms}, which is 2 to 3 times higher than the rated ripple-current. Without effective thermal management, high current can significantly decrease capacitor life. Since capacitor life depends on its temperature, which is affected by 1) self-heating caused by capacitor's ESR and ripple current, 2) ambient temperature and 3) other heat sources, which in this study are the bus bars. Figure 11 shows how capacitor life is affected by the capacitor core temperature and the core temperature increase caused by ripple current.

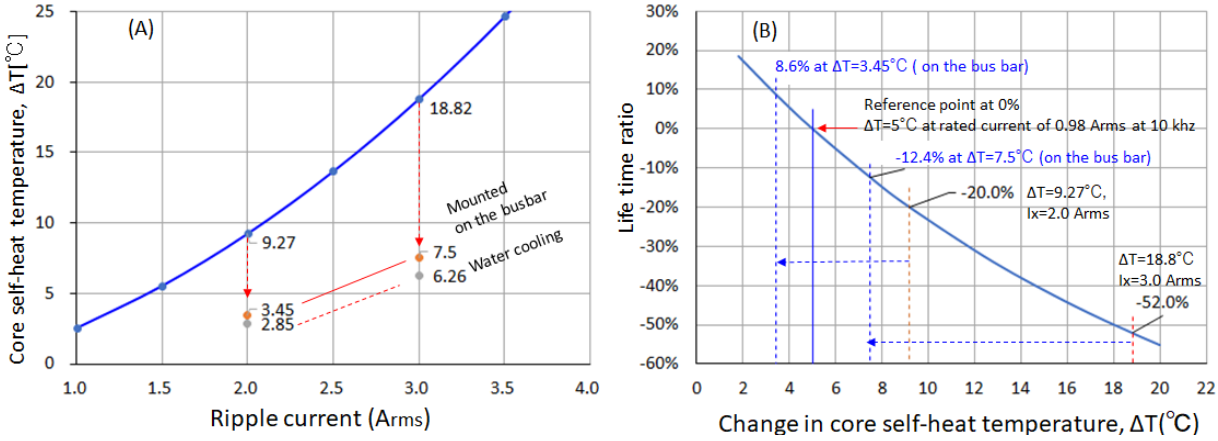

Figure 11: (A) Increase in capacitor core temperature as a function of the applied ripple current. (B) Change in capacitor life as a function of capacitor core temperature relative to 5 ºC self-heating at the rated ripple current for the HXC series 82 µF/63 V capacitor.

Figure 11A shows that a ripple current increase from 2 to 3 A_{rms} increases the core temperature of a single unmounted capacitor from 9.27 to 18.82 ºC. Experimental measurements when the capacitors were mounted on the bus bar showed the highest temperature rise for a capacitor was only ΔT=3.45 ℃ at 2 A_{rms} and ΔT = 7.5 ℃ at 3 A_{rms}. The self-heat is removed through the new concept bus bar, which functions as a heat sink. Additional experimental measurements showed the highest temperature rise for a capacitor was only ΔT = 2.85 ℃ at 2 A_{rms} and ΔT = 6.26 ℃ at 3 A_{rms} when the bus bar module was water cooled.

Figure 11B shows capacitor life is decreased 20% for a core temperature rise of 9.27 ℃, i.e. at 2 A_{rms} and decreased 52% for a core temperature rise of 18.8 ℃, i.e. at 3 A_{rms}. With a ripple current of 3 A_{rms}, life improves from a 52% decrease to only a 12.4% decrease when the capacitors are mounted on the new concept bus bar. A key point for thermal management of the module is to properly reduce the negative effects of self-heating.

2.3 Thermal simulation of the 48-capacitor Module with Thermal Management

Experimental measurements and thermal simulation results for the 48-capacitor module are compared with and without water cooling. The experimental setup is shown in Figure 12. Thermocouples are mounted on selected capacitors and on the bus bar. The module was then installed in a test box that was mounted in a chamber held at 25 ºC. The temperature of each capacitor depends on its self-heating, which is influenced by radiation from neighboring capacitors and the bus bar.

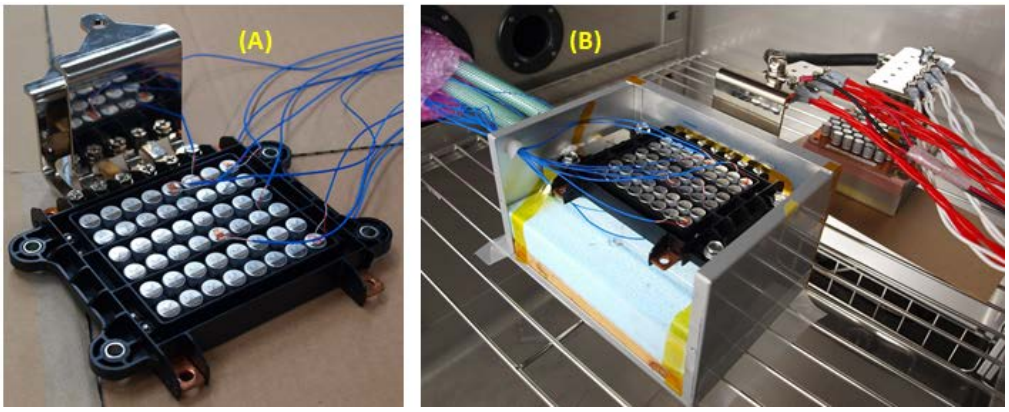

Figure 12: (A) 48 capacitors in the test module with thermocouples on selected capacitors (B) the module is installed in a test box, which was closed with covers on the top and sides and placed in a larger chamber held at 25 ^{o}C during testing. The module is sitting on a water jacket, which in turn is sitting on Styrofoam. Details on the water jacket and foam are shown later.

Testing was performed with and without water cooling. Results of thermal simulation and measurements with no water cooling are shown in Figure 13 with 90 A_{rms} ripple-current applied. The temperature outside the test box was held at 25 ℃ and the air temperature inside the box rose to 33 ℃. The simulation accurately predicted the measurements with the coolest capacitor at ~38.1 ^{o}C and the hottest capacitor at ~ 39.6 ^{o}C.

The triangular current input terminal bus bar plate sits outside the test box and it functioned like a heat sink. The maximum temperature difference for capacitors along the horizontal direction was 1.8 ℃ and along the vertical direction it is 3.7 ℃. This is shown in greater detail in Figure 14, where temperatures of individual capacitors are shown along the horizontal and the vertical lines that are shown in Figure 13B.

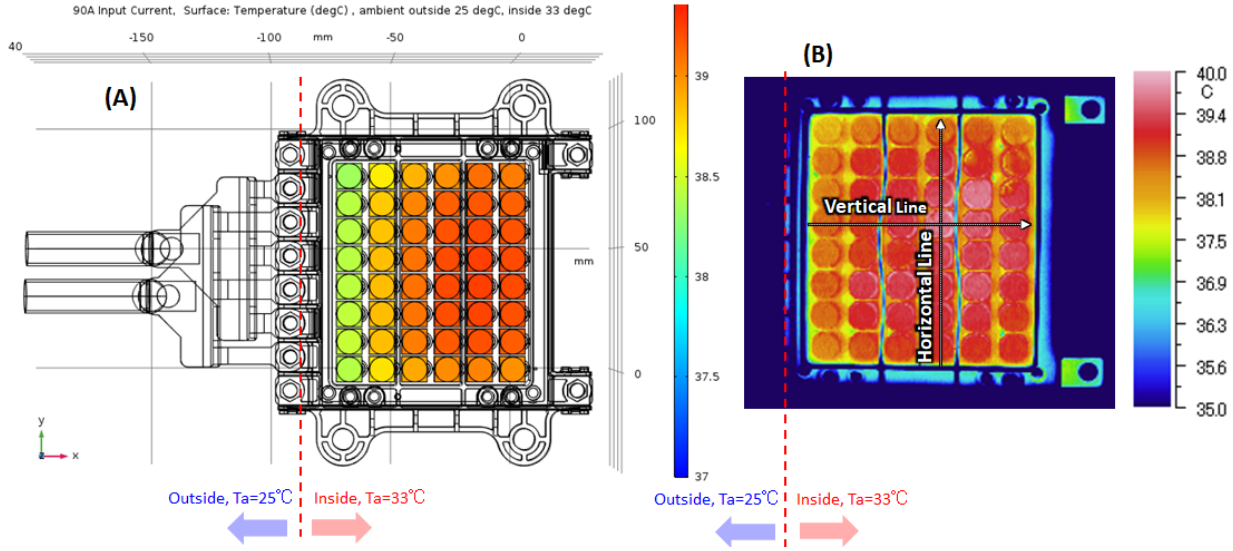

Figure 13: (A) Thermal simulation temperature predictions for a ripple-current of 90 A_{rms}. (B) Measured temperatures for a ripple current of 90 A_{rms}. Note that colors of the two thermal scales are not the same. Simulation and measurements agree quite well.

When the module and terminal bus bar plate are at the same temperature, i.e. both in the test box, the terminal bus bar does not remove heat and capacitors near the terminal are at a higher temperature because the highest current densities are at that location. The effect of having higher current densities is shown by thermal simulation in Figure 15. A wide-angle current input terminal as shown improves current density uniformity and clearly improves the thermal uniformity. Area (A) shown in Figure 15 is slightly higher temperature (less than 1°C) than area (B).

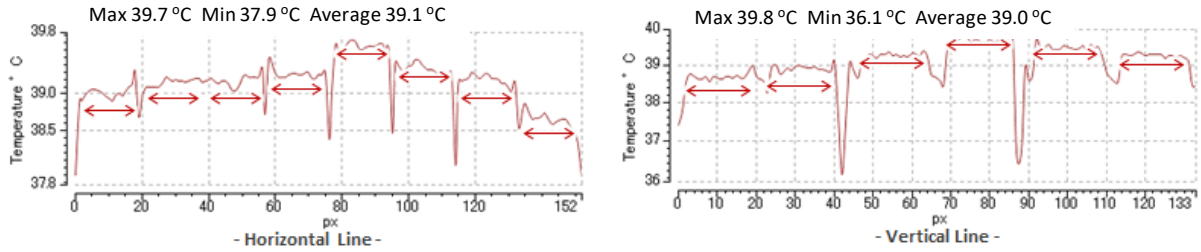

Figure 14: Left – Temperatures measured by thermograpy for the eight capacitors along the line labeled "horizontal" in Figure 13B. Right – Temperatures measured by thermography for the six capacitors along the line labelled "vertical" in Figure 13B.

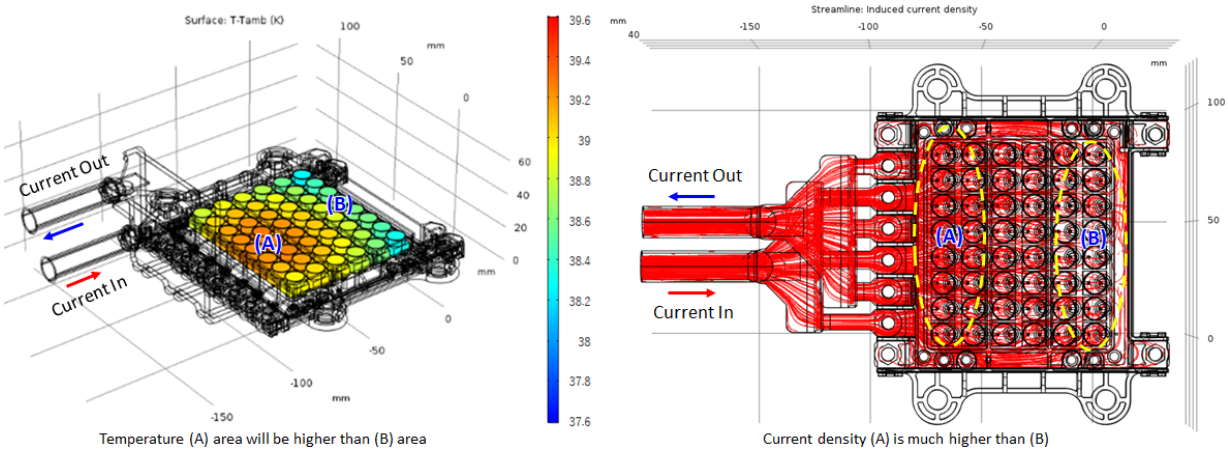

Figure 15: Capacitor temperatures with a wide-angle current input terminal calculated by thermal simulation. Capacitors show improved temperature uniformity but those near the terminals do experience more self-heating because of higher current densities.

The effect of water cooling the module is shown in Figure 16. Water temperature was 15 °C with a flow rate of 6 liters/minute. The module was cooled from below where it contacted the cooled water jacket. The maximum temperature differences for capacitors along the horizontal and vertical directions are similar to those measured without water cooling but the average capacitor temperature is below 20 °C rather than above 39 °C. The temperature of capacitors near the input terminal is slightly higher in this configuration because temperatures inside the box are < 20 ℃ and the chamber temperature is 25 ℃.

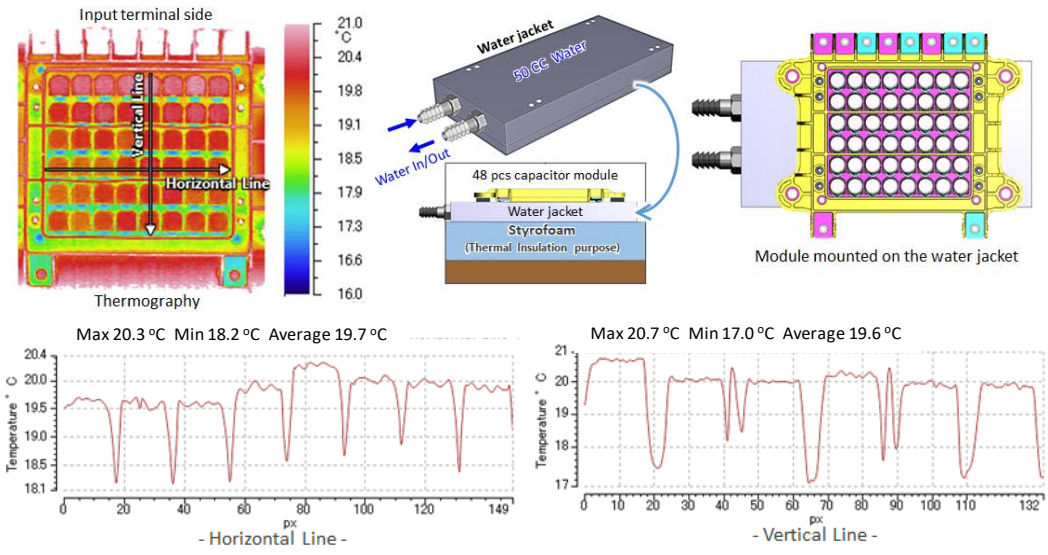

Figure 16: Experimental results for capacitor temperatures when the module is sitting on a water-cooled jacket with 15 °C water flowing at 6 liters/minute. The applied ripple current was 90 A_{rms}.

3 Life Analysis

Capacitor life can be expressed as

$$L(\Delta T_x, T_a) = L_o \cdot K_1^{K_2[(To-Ta)+(\Delta To-\Delta Tx)]} \quad (3)$$

where ΔT_x is the temperature rise due to capacitor self-heating, ΔTo is the self-hest at the rated ripple current, T_a is the ambient temperature, T_o is the rated temperature of the capacitor, and K_1 and K_2 are experimentally determined constants. If all capacitors in a module are at rated temperature T_o, then the life is Lo. When each capacitor in a module has a different temperature, module life can be calculated using Miner's Rule [5].

$$L(\text{module}) = 1 \Big/ \sum_{n=1}^{m} \frac{Rn}{Ln} \quad (4)$$

where Rn is the fraction of capacitors at each of the m temperatures and Ln is capacitor life at temperature n.

Life analysis for the 48-capacitor module must take into account capacitor manufacturing variability. Capacitors do have a ripple current rating but the effect of ripple current is more complex. When 48 capacitors are connected in parallel, the ripple current seen by each capacitor depends on its impedance. Because of manufacturing variability, there is a distribution in the properties of the 48 capacitors. The impedance for a C = 82 μF capacitor (the design center value) operating at f = 10 kHz is 194 mΩ. That is, $Xc = 1/(2 \cdot \pi \cdot f \cdot C) = 194$ mΩ, which is much greater than the average ESR production value of ~24.65 mΩ. Thus, the distribution of capacitance values determines the distribution of ripple currents among the 48 capacitors.

A worst case scenario is examined. Assume a module consists of 16 capacitors with +20% capacitance values and the highest ESR of 28.88 mΩ and 32 capacitors with -20% capacitance values and an average ESR = 24.65 mΩ. The ESR values are from production data for 23,000 pieces. The average ESR (μ) is 24.65 mΩ and the maximum value is 28.88 mΩ (μ+4σ value obtained from the distribution). Table 4 shows parameters for this worst case scenario analysis. Heat loss from self-heating also results in power loss, as listed.

Table 4: Capacitor properties for a worst case scenario in a 48-capacitor module where production variability is included. Input ripple current is 90 A_{rms}.

Number of capacitors	Tolerance (capacitance of each piece (μF))	ESR (mΩ)	Ix, Current/capacitor (A_{rms})	Total self-heating (W)	Relative self-heating (%)
16	+20% (98.6)	28.88	2.41 note1	2.68 note 2	56.8
32	-20% (65.6)	24.65	1.61	2.04	43.2

Note 1- Capacitance of the 16 capacitors in parallel is 98.6 μF x 16 =1574.4 μF and of the 32 capacitors the value is 2099.3 μF. Total current to the 16 capacitors =[90 A_{rms}*1574.4/(1574.4+2099.3)]/16 = 2.41 A_{rms}.
Note 2 –power loss = I^2*ESR = 2.41 A_{rms}^2*28.88 mΩ*16 = 2.68 W.

Module life predicted for this worst case scenario is next calculated. For the operating temperature profile shown in Figure 17 with ambient temperatures from 40 to 120℃, predicted life of the module is calculated at each ambient temperature as shown in Table 4 then equation 4 is used to calculate module life.

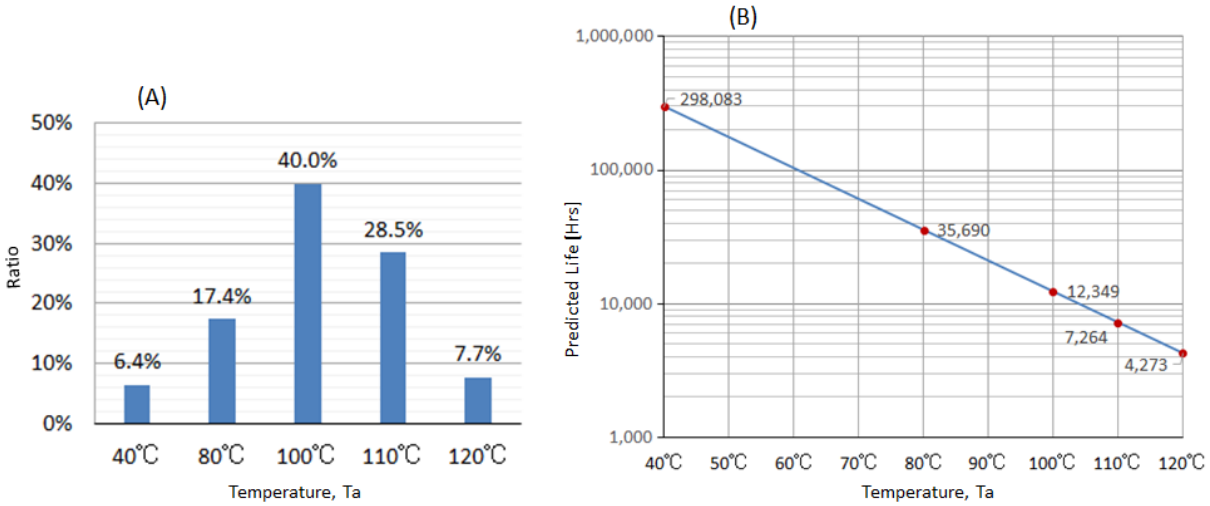

Figure 17: (A) Temperature profile with percentage of time at each temperature. (B) Module life calculated with the assumed worst case scenario manufacturing variability.

Table 4: Predicted module life for a ripple current of 90 A_{rms} and the operating temperature profile of Figure 17A.

Ix	Fraction of total (%)	Life (hours) at each temperature (Ta) condition				
		40℃	80℃	100℃	110℃	120℃
2.41 A_{rms}	56.8	261,880	31,355	10,849	6,382	3,754
1.61 A_{rms}	43.2	364,279	43,615	15,092	8,878	5,222
Combined total L_{TA}		298,083*[1)]	35,690	12,349	7,264	4,273

*1) at Ta = 40 ºC L_{TA} = 1/(0.568/261,880 + 0.432/364,279) = 298,083 Hrs

The predicted module life for the Figure 17 temperature profile is:

L = 1/(0.064/298,083 + 0.174/35,690 + 0.4/12,349 + 0.285/7,264 + 0.077/4,273) = 10,555 Hrs.

The typical life requirment of a passenger vehicle is 8,000~9,000 hours. Thus, predicted life for the new concept bus bar containing 48 Nippon Chemi-Con HXC capacitors meets the requirements of this application.

4. Conclusion

We described a new design for the DC-link-capacitor module used in 48-V hybrid passenger vehicles. This design uses low-profile hybrid-polymer aluminium electrolytic capacitors mounted within a patent pending package that efficiently handles heat generated by the high ripple currents. Thermal management and packaging details were reported with thermal simulation results that are compared with actual temperature measurements. Life of the new concept module is predicted to exceed passenger vehicle life.

Acknowledgments

We thank Kentaro Nakaaki, Kouji Yamaya, Osamu Ichikura, Naohisa Shibata at the Solution Development Department and Yuki Arai at the Products Development Department-II Team at Nippon Chemi-Con, Japan. We also thank Dr. Gopal P. Mathur and Kevin Elmer at Meta Acoustic Technology, LLC for their thermal simulation support.

References

[1] Brian Sisk, PhD, A123,*"Is there One Solution for Batteries Suporting 48-V Mild Hybrid?"*, Electric & Hybrid Vehicle Technology Conference 2018, September 12-13, 2018.

[2] https://www.theicct.org/sites/default/files/publications/ICCT_Post-2020-CO2-stds-EU_briefing_20171026_rev20171129.pdf,accessed on 10-25-2018.

[3] Matti Vint, *"Do 48V Powertrains Makes Sense for The North American Market"*, Electric & Hybrid Vehicle Technology Conference 2018, September 12-13, 2018.

[4] https://www.polarinstruments.com/support/cits/AP144.html, accessed on 10-25-2018.

[5] Nian-Zhong Chen, Ge Wang, and C. Guedes Soares, "*Palmgren–Miner's rule and fracture mechanics-based inspection planning*", Engineering Fracture Mechanics, Volume 78, Issue 18, December 2011, pages 3166–3182.

Authors

Toshihiko Furukawa earned his EE degree from Tokai University in Japan and has more than 20 years of experience in power electronics and high-frequency amplifier design. He currently is focused on capacitor technology, providing technical support and global-market business development for United Chemi-Con / Nippon Chemi-Con Group. IEEE Membership 92515077 and SAE Membership 6125613949.

Yuya Tamai earned his Master's degree in electrical engineering from Oita University in Japan and has 15 years of experience at Nippon Chemi-Con Corporation, Solution R&D Department. His focus is on capacitor module design, circuit design/simulation and thermal design for the automotive field.

Yuhei Kobayashi earned his Master's degree in mechanical engineering from Muroran Institute of Technology in Japan and has more than five years of experience at Nippon Chemi-Con Corporation, Solution R & D Department. His focus is on mechanical design and thermal simulation.

Toshiki Wakabayashi earned his Master's degree in applied chemistry from Tokyo University of Agriculture and Technology in Japan and has 17 years of experience at Nippon Chemi-Con Corporation, Products R&D Department. His focus is on the design and development of conductive polymer hybrid aluminium electrolytic capacitors.